The hydrogen atoms were located from a difference Fourier. Anisotropic refinement of all nonhydrogen atoms and hydrogen positional parameters (isotropic B value at one more than average value of ring carbons and boron atoms) yielded a final $R_1 = 0.0428$ and $R_2 = 0.0408$. (Convergence was considered complete when all the shifts were less than one-tenth their standard deviation.) Here $R_1 = \sum||F_o| - |F_c||/\sum|F_o|$, $R_2 = [\sum w(|F_o| - |F_c|)^2/\sum wF_o^2]^{1/2}$, $w = 1/\sigma(F_o)^2$, $\sigma(F_o) = \sigma(F_o^2)/2F_o$, $F_o^2 = F^2/Lp$, and $\sigma(F_o^2) = [\sigma(I_{raw})^2 + (0.25F^2)^2]^{1/2}/Lp$.

The function minimized was $\sum w|F_o| - |F_c|)^2$. Atomic scattering factors for all atoms were taken from the compilation of Cromer and Waber[22] and were corrected for anomalous dispersion (both real and imaginery parts).[22]

Final positional and thermal parameters are presented in Table I. A table of observed and calculated structure factors is available as supplementary material (Table V). Inclusion of the unobserved reflections had little or no effect on the bond distances and angles. The final difference map was relatively smooth with maxima of ±0.345 e/Å^3 in the region of the P–N bonds.

Acknowledgment. This work was supported by N.A.S.A., Ames Research Center.

Supplementary Material Available: A listing of structure factor amplitudes for IV (17 pages). Ordering information is given on any current masthead page.

(22) Cromer, D. T.; Waber, J. T. "International Tables for X-Ray Crystallography"; The Kynoch Press: Birmingham, England, 1974; Vol. IV, Tables 2.2 B and 2.31.

Structures of $[(CH_3)_2(t\text{-BuN})W]_2(\mu\text{-}t\text{-BuN})_2$ and $[((CH_3)_2N)_2Ti]_2(\mu\text{-}t\text{-BuN})_2$. A Molecular Orbital Explanation of the Existence of Unsymmetrically or Symmetrically Bridging Organoimido Ligands

David. L. Thorn,* William A. Nugent,* and Richard L. Harlow

Contribution No. 2766 from the Central Research and Development Department, E. I. du Pont de Nemours and Company, Experimental Station, Wilmington, Delaware 19898.
Received April 11, 1980

Abstract: The crystal structures of the unsymmetrically bridging imido complex $[(CH_3)_2(t\text{-BuN})W]_2(\mu\text{-}t\text{-BuN})_2$ (Ib) and the symmetrically bridging imido complex $[((CH_3)_2N)_2Ti]_2(\mu\text{-}t\text{-BuN})_2$ (IIb) have been determined. Both compounds Ib and IIb crystallize in the space group $P2_1/n$ with two molecules in the unit cell. Compound Ib has the cell dimensions (at −100 °C) $a = 12.987$ (2) Å, $b = 9.477$ (2) Å, $c = 11.252$ (2) Å, $\beta = 103.85$ (1)°, $V = 1345$ Å^3, and $\rho_{calcd} = 1.759$ g cm^{-3}; compound IIb has the cell dimensions (at −20 °C) $a = 9.434$ (2) Å, $b = 15.984$ (4) Å, $c = 8.795$ (2) Å, $\beta = 115.55$ (2)°, $V = 1197$ Å^3, and $\rho_{calcd} = 1.150$ g cm^{-3}. Final conventional and weighted agreement indices on F_o for $F_o^2 > 3\sigma(F_o^2)$ are 0.033 and 0.031 for Ib and 0.040 and 0.037 for IIb. Molecular orbital calculations suggest that the unsymmetrical bridging mode in Ib, and in the previously studied Mo analogue Ia, is a manifestation of an "antiaromatic" electronic structure and that the symmetrical bridging mode in IIb and in the previously examined Zr analogue IIa is consistent with an "aromatic" electronic structure.

Transition-metal imido (NH and NR) species are ubiquitous intermediates in industrial[1] and laboratory[2] organic synthesis. Nevertheless, our systematic understanding of the chemistry of imido compounds is limited, particularly with regard to the relationship between structure and reactivity.[3] Structural studies in these laboratories[4] and elsewhere[3] have established that five different bonding modes (1–5) can be present in these complexes. An understanding of the electronic differences reflected by modes

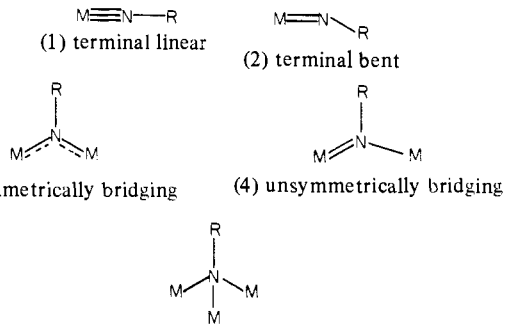

1–5 should provide insight into the chemistry of the respective complexes. Moreover such an investigation should also shed light on structure-reactivity trends in the related alkylidene[5] and oxo[6] transition-metal complexes.

Recently we have isolated and structurally characterized the imido-bridged dimeric compound $[(CH_3)_2(t\text{-BuN})Mo]_2(\mu\text{-}t\text{-BuN})_2$ (Ia),[4f] drawn below. The distinctly asymmetric structure in the bridging region of Ia[4f] is remarkably different from the symmetrical structure of the imido-bridged dimer $[((CH_3)_2N)_2Zr]_2(\mu\text{-}t\text{-BuN})_2$ (IIa).[4d] This difference has prompted us to determine the structures and establish the mode of bridge bonding in the

(1) Examples of such reactions and relevant literature include the following. (a) Ammoxidation of propylene to acrylonitrile: Burrington, J. D.; Grasselli, R. K. *J. Catal.* **1979**, *59*, 79–99. (b) Hydrogenation of nitriles: Andrews, J. A.; Kaesz, H. D. *J. Am. Chem. Soc.* **1977**, *99*, 6763–6765. (c) Haber ammonia synthesis: Jones, A.: McNicol, B. D. *J. Catal.* **1977**, *47*, 384–388; Irgranova, E. G.; Ostrovskii, V. E.; Temkin, M. I. *Kinet. Katal.* **1976**, *17*, 1257–1262.

(2) Examples include the following. (a) Osmium-catalyzed oxyamination of olefins: Sharpless, K. B.; Chong, A. O.; Oshima, K. *J. Org. Chem.* **1976**, *41*, 177–179; Herranz, E.; Sharpless, K. B. *Ibid.* **1978**, *43*, 2544–2548; Herranz, E.; Biller, S. A.; Sharpless, K. B. *J. Am. Chem. Soc.* **1978**, *100*, 3596–3598. (b) Electrochemical tosylamidation at a vanadium anode: Breslow, R.; Kluttz, R. Q.; Khanna, P. L. *Tetrahedron Lett.* **1979**, 3273–3274. (c) Reduction of organic azides: Ho, T.-L.; Henninger, M.; Olah, G. A. *Synthesis* **1976**, 815–816; Kwart, H.; Kahn, A. A. *J. Am. Chem. Soc.* **1967**, *89*, 1950–1950.

(3) For a review on organoimido and related complexes of transition metals see: Nugent, W. A.; Haymore, B. L. *Coord. Chem. Rev.* **1980**, *31*, 123–175.

(4) (a) Nugent, W. A.; Harlow, R. L. *J. Chem. Soc., Chem. Commun.* **1978**, 579–580. (b) *Ibid.* **1979**, 342–343. (c) *Ibid.* **1979**, 1105–1106. (d) *Inorg. Chem.* **1979**, *18*, 2030. (e) *Ibid.* **1980**, *19*, 777–779. (f) *J. Am. Chem. Soc.* **1980**, *102*, 1759–1760. (g) Nugent, W. A.; Harlow, R. L.; McKinney, R. J. *Ibid.* **1979**, *101*, 7265–7268.

(5) Schrock, R. R. *Acc. Chem. Res.* **1979**, *12*, 98–104.

(6) Griffith, W. P. *Coord. Chem. Rev.* **1970**, *5*, 459–517.

0002-7863/81/1503-357$01.00/0

Chart I

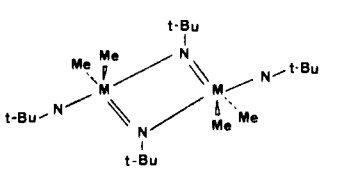

Ia, M = Mo
Ib, M = W

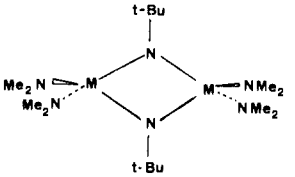

IIa, M = Zr
IIb, M = Ti

related compounds $[(CH_3)_2(t\text{-BuN})W]_2(\mu\text{-}t\text{-BuN})_2$ (Ib) and $[((CH_3)_2N)_2Ti]_2(\mu\text{-BuN})_2$ (IIb).[7] We find that the titanium complex IIb is isostructural with its Zr analogue IIa and has a symmetrically bridged structure and that the tungsten complex Ib is isostructural with the Mo complex Ia and possesses the unsymmetrical bridging structure.[8] In this paper we report the X-ray crystal structures of Ib and IIb. The persistence of the different bridging modes in compounds I and II has encouraged us to probe the electronic causes of the asymmetry in the compounds Ia,b. Our ultimate conclusion, upon which we elaborate in the remainder of this paper, is conveniently summarized in the representations of I and II illustrated in Chart I. The bridging region of II is, electronically, a delocalized, "aromatic" system and has the requisite equal bond lengths, while the bridging region of I is "antiaromatic" and prefers a localized bonding system of alternating long–short bond lengths.[9] It is not at all obvious how this difference can arise between two complexes which are, at first glance, electronically very similar; both are formally d^0 metal compounds and are nominally isoelectronic in the bridging region. However, the different natures and locations of the terminal ligands result in significantly different bonding in the bridging regions in the two complexes, and it is these effects which we wish to examine.

The factors responsible for establishing the geometries of ligand-bridged metal dimers have been discussed by several workers,[10] notably Dahl and colleagues[11] and Hoffmann and co-workers.[12] However, the specific geometrical issue which we are addressing, the question of why a dimer will have a distinctly unsymmetrical bridging structure when closely related structures of high symmetry are intuitively and experimentally realizable, has to our knowledge not been previously studied.[13] In this paper we will confine our attention to the imido-bridged compounds I and II and close structural analogues thereof.

(7) This complex was originally reported by: Bradley, D. C.; Torrible, E. G. *Can. J. Chem.* **1963**, *41*, 134–138.

(8) All the compounds (Ia, Ib, IIa, IIb) have crystallographically imposed inversion centers and no other exact symmetry. There remain two crystallographically independent metal–N(bridge) separations. By "unsymmetrical" we mean the significant nonequivalence of these two independent separations in I (a and b), and by "symmetrical" we mean the equivalence of these independent separations in II (a and b).

(9) Aromaticity and antiaromaticity are used here in the sense of a "delocalized" or "localized" bonding system. See: Thorn, D. L.; Hoffmann, R. *Nouv. J. Chim.* **1979**, *3*, 39–45 and references therein. See also: Goldstein, M. J.; Hoffmann, R. *J. Am. Chem. Soc.* **1971**, *93*, 6193–6204. We have not yet examined these compounds for other manifestations of their "aromaticity" or "antiaromaticity", e.g., ring currents.

(10) (a) Mason, R.; Mingos, D. M. P. *J. Organomet. Chem.* **1973**, *50*, 53–61. (b) Burdett, J. K. *J. Chem. Soc., Dalton Trans.* **1977**, 423–428. (c) Norman, J. G.; Gmur, D. J. *J. Am. Chem. Soc.* **1977**, *99*, 1446–1450.

(11) (a) Dahl, L. F.; deGil, E. R.; Feltham, R. D. *J. Am. Chem. Soc.* **1969**, *91*, 1653–1664. (b) Teo, B. K.; Hall, M. B.; Fenske, R. F.; Dahl, L. F. *J. Organomet. Chem.* **1974**, *70*, 413–420. (c) Teo, B. K.; Hall, M. B.; Fenske, R. F.; Dahl, L. F. *Inorg. Chem.* **1975**, *14*, 3103–3117 and references therein.

(12) (a) Hay, P. J.; Thibeault, J. C.; Hoffmann, R. *J. Am. Chem. Soc.* **1975**, *97*, 4884–4899. (b) Summerville, R. H.; Hoffmann, R. *Ibid.* **1976**, *98*, 7240–7253. (c) Summerville, R. H.; Hoffmann, R. *Ibid.* **1979**, *101*, 3821–3831. (d) Pinhas, A. R.; Hoffmann, R. *Inorg. Chem.* **1979**, *18*, 654–658. (e) Dedieu, A.; Albright, T. A.; Hoffmann, R. *J. Am. Chem. Soc.* **1979**, *100*, 3141–3151.

(13) An interesting but unrelated issue is the question of unsymmetrically bridging hydride ligands. See for example: Roziere, J.; Williams, J. M.; Stewart, R. P., Jr.; Peterson, J. L.; Dahl, L. F. *J. Am. Chem. Soc.* **1977**, *99*, 4497–4499; Peterson, J. L.; Johnson, P. L.; O'Connor, J.; Dahl, L. F.; Williams, J. M. *Inorg. Chem.* **1978**, *17*, 3460–3469; Bau, R.; Teller, R. G.; Kirtley, S. W.; Koetzle, T. F. *Acc. Chem. Res.* **1979**, *12*, 176–183.

Table I. Summary of the Crystal Data for the Two Crystallographic Studies

	Ib	IIb
mol formula	$C_{20}H_{48}N_4W_2$	$C_{16}H_{42}N_6Ti$
mol wt	712.33	414.35
cryst dimens, mm	0.30 × 0.21 × 0.30	0.30 × 0.19 × 0.40
cryst temp, °C	−100	−20
crystal system	monoclinic	monoclinic
space group	$P2_1/n$	$P2_1/n$
unit cell		
a, Å	12.987 (2)	9.434 (2)
b, Å	9.477 (2)	15.984 (4)
c, Å	11.252 (2)	8.795 (2)
β, deg	103.85 (1)	115.55 (2)
cell vol, Å^3	1345	1197
Z	2	2
calcd density, g cm^{-3}	1.759	1.150
abs coeff, cm^{-1}	90.7	7.01

Table II. Summary of the Refinement of the Two Structures

	Ib	IIb
no. of reflctns with $I > 2\sigma(I)$	2298	2043
no. of variables	188	193
hydrogen atoms	not refined	refined
R^a	0.033	0.040
$R_w{}^b$	0.031	0.037
peaks in final difference Fourier	four (0.39–0.69 e Å^{-3}) near W	0.29, 0.35 e Å^{-3} near N(1), Ti

$^a R = \Sigma||F_o| - |F_c||/\Sigma|F_o|$. $^b R_w = [\Sigma w(|F_o| - |F_c|)^2/\Sigma w|F_o|^2]^{1/2}$.

Table III. Selected Bond Distances and Angles for Compound Ib

Bond Distances (Å) with Estimated Standard Deviations			
W-W	3.093 (1)	N(2)-C(21)	1.488 (7)
W-N(1)	1.736 (5)	C(11)-C(12)	1.495 (9)
W-N(2)	1.842 (4)	C(11)-C(13)	1.531 (10)
W-N(2)'	2.288 (5)	C(11)-C(14)	1.500 (10)
W-C(1)	2.163 (6)	C(21)-C(22)	1.537 (8)
W-C(2)	2.171 (5)	C(21)-C(23)	1.525 (8)
N(1)-C(1)	1.465 (7)	C(21)-C(24)	1.523 (8)
Bond Angles (Deg) with Estimated Standard Deviations			
N(1)-W-N(2)	108.3 (2)	N(1)-C(11)-C(12)	110.0 (5)
N(1)-W-N(2)'	168.1 (2)	N(1)-C(11)-C(13)	107.4 (6)
N(1)-W-C(1)	92.6 (2)	N(1)-C(11)-C(14)	108.9 (6)
N(1)-W-C(2)	92.4 (2)	C(12)-C(11)-C(13)	110.1 (7)
N(2)-W-N(2)'	83.6 (2)	C(12)-C(11)-C(14)	110.8 (8)
N(2)-W-C(1)	111.2 (2)	C(13)-C(11)-C(14)	109.6 (7)
N(2)-W-C(2)	109.7 (2)	N(2)-C(21)-C(22)	110.6 (5)
N(2)'-W-C(1)	82.4 (2)	N(2)-C(21)-C(23)	108.7 (5)
N(2)'-W-C(2)	83.7 (2)	N(2)-C(21)-C(24)	110.0 (5)
C(1)-W-C(2)	134.7 (2)	C(22)-C(21)-C(23)	109.7 (5)
W-N(1)-C(11)	168.3 (4)	C(22)-C(21)-C(24)	108.2 (5)
W-N(2)-W'	92.4 (2)	C(23)-C(21)-C(24)	109.7 (6)
W-N(2)-C(21)	134.2 (4)		
W'-N(2)-C(21)	129.4 (3)		

Experimental Section

Structural Details. The methods used for the preparations of compounds Ib and IIb have been described previously.[4d,f] Crystals of both Ib and IIb were mounted in glass capillaries and placed on a Syntex P3 diffractometer (graphite monochromator, Mo Kα radiation, λ = 0.71069 Å). The crystal system, space group, and approximate unit cell dimensions of each crystal were determined during a preliminary investigation. The quality of both crystals was found to be adequate on the basis of ω scans which showed the peak width at half-height to be ca. 0.21 and 0.25°, respectively. The unit-cell dimensions were subsequently refined from the Bragg angles of 50 computer-centered reflections. A summary of the crystal data is given in Table I.

Intensity data were collected by using the ω-scan technique (4° < 2θ < 55°; variable scan rate of 2.0–5.0° min^{-1}; total background time equal to scan time). Scan widths for Ib and IIb were 1.0 and 0.8°, respectively. For IIb, 2756 reflections were recorded at −20 °C and for Ib, 3089

Table IV. Selected Bond Distances and Angles for Compound IIb

Bond Distances (Å) with Estimated Standard Deviations			
Ti--Ti'	2.804 (1)	N(2)-C(5)	1.451 (3)
Ti-N(1)	1.921 (2)	N(2)-C(6)	1.446 (3)
Ti-N(1)'	1.925 (2)	N(3)-C(7)	1.450 (3)
Ti-N(2)	1.914 (2)	N(3)-C(8)	1.443 (3)
Ti-N(3)	1.913 (2)	C(1)-C(2)	1.525 (3)
N(1)-C(1)	1.481 (2)	C(1)-C(3)	1.516 (3)
		C(1)-C(4)	1.510 (3)
Bond Angles (Deg) with Estimated Standard Deviations			
N(1)-Ti-N(1)'	86.39 (7)	C(5)-N(2)-C(6)	110.9 (2)
N(1)-Ti-N(2)	114.49 (7)	Ti-N(3)-C(7)	124.3 (2)
N(1)-Ti-N(3)	114.05 (7)	Ti-N(3)-C(8)	125.2 (2)
N(1)'-Ti-N(2)	114.30 (7)	C(7)-N(3)-C(8)	111.3 (2)
N(1)'-Ti-N(3)	114.48 (7)	N(1)-C(1)-C(2)	108.8 (2)
N(2)-Ti-N(3)	111.17 (7)	N(1)-C(1)-C(3)	109.9 (2)
Ti-N(1)-Ti'	93.61 (7)	N(1)-C(1)-C(4)	110.0 (2)
Ti-N(1)-C(1)	129.6 (1)	C(2)-C(1)-C(3)	109.6 (3)
Ti'-N(1)-C(1)	131.0 (1)	C(2)-C(1)-C(4)	109.4 (3)
Ti-N(2)-C(5)	120.9 (2)	C(3)-C(1)-C(4)	109.2 (3)
Ti-N(2)-C(6)	127.8 (2)		

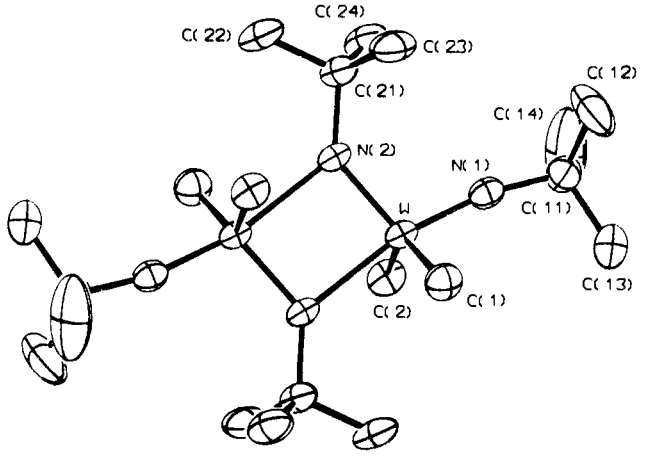

Figure 1. Structure of Ib, $[(CH_3)_2(t\text{-BuN})W]_2(\mu\text{-}t\text{-BuN})_2$, showing the numbering scheme. Thermal ellipsoids are drawn at the 50% probability level here and in Figure 2.

reflections at −100 °C. The intensities of four standard reflections were monitored periodically; only statistical fluctuations were noted. The intensities of several reflections were measured in 10° increments about the diffraction vector; as a result, empirical corrections for absorption were applied (factors ranged 0.93–1.00 for IIb and 0.44–1.00 for Ib).

The solution and refinement of the structures were carried out on a PDP-11 computer by using local modifications of the programs supplied by the Enraf-Nonius Corp.[14] The atomic scattering factors were taken from the tabulations of Cromer and Waber;[15a] anomalous dispersion corrections were by Cromer.[15b] In the least-squares refinement, the function minimized was $\sum w(|F_o| - |F_c|)^2$ with the weights w assigned as $1/\sigma^2(F_o)$. The standard deviations of the observed structure factors, $\sigma(F_o)$, were based on counting statistics and an "ignorance factor" p of 0.02.[16]

The structure of IIb was solved by direct methods (MULTAN). Solution of the structure of Ib was facilitated by the availability of the structure of Ia to which it is isomorphous. Both structures were refined by the full-matrix least-squares method. All of the nonhydrogen atoms in both structures were refined with anisotropic thermal parameters. The hydrogen atoms in Ib were included but not refined; hydrogen atoms in IIb were refined with isotropic thermal parameters. The results are summarized in Table II. Important bond distances and angles are summarized for Ib in Table III and for IIb in Table IV.

(14) Frenz, B. A. "Computing in Crystallography"; Schenk, H., Olthof-Hazehamp, R., van Koningsveld, H., Gassi, G. C., Eds.; Delft University Press: Delft, Holland, 1978; pp 64–71.

(15) (a) "International Tables for X-ray Crystallography"; Kynoch Press: Birmingham, England, 1974; Vol. 4, Table 2.2B. (b) *Ibid.*, Table 2.3.1.

(16) Corfield, P. W. R.; Doedens, R. J.; Ibers, J. A. *Inorg. Chem.* **1967**, *6*, 197–204.

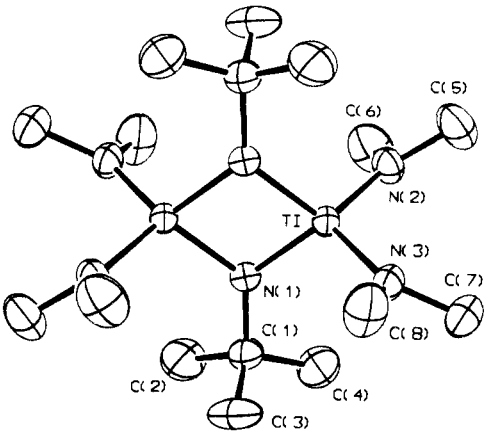

Figure 2. Structure of IIb, $[((CH_3)_2N)_2Ti]_2(\mu\text{-}t\text{-BuN})_2$.

Results and Discussion

Description of the Structures. Drawings of the compounds Ib and IIb are presented in Figures 1 and 2, respectively. Selected bond distances and angles are listed in Tables III and IV. The atomic coordinates are listed in Tables V and VI. Tables of structure factor amplitudes, hydrogen atom positions, and least-squares planes (IIb only) are available as supplementary material.

The structure of Ib is exactly analogous to the structure of the Mo complex Ia and is the second example of a complex with unsymmetrically bridging imido ligands.[8] As in Ia[4f] the dimeric molecule is situated on a crystallographic inversion center. The local coordination about each tungsten atom is distorted trigonal bipyramidal, with the three equatorial sites occupied by two methyl ligands and a nominally doubly bonded bridging imido nitrogen atom N(2) (see Figure 1) and the two axial sites occupied by a triply bonded terminal imido nitrogen atom N(1) and a singly bonded bridging imido nitrogen atom N(2)′. The corresponding W–N distances (see Table III; W–N(1) = 1.736 (5) Å, W–N(2) = 1.842 (4) Å, W–N (2)′ = 2.288 (5) Å) are consistent with the assigned bond character. The larger W–N bridge separation is much longer than might be expected (ca. 1.98 Å[17]) for a sp^2-hybridized N–W single bond with possible π interactions. This may be the result of a trans effect from the terminal alkylimido ligand, in addition to the electronic effects which are discussed below.

Likewise, the structure of IIb is analogous to the previously published structure of the Zr complex IIa.[4d] Again each dimer is situated on a crystallographic inversion center. Each titanium atom is tetrahedrally coordinated by two nearly planar terminal amido ligands and two slightly pyramidal bridging imido ligands. The carbon atom which is bonded to the bridging imido nitrogen, atom C(1), lies 0.487 (2) Å from the plane defined by the titanium and bridging imido nitrogen atoms. Within experimental error the two independent bridging nitrogen to titanium atom distances are equal (see Table IV).

Simple Hückel Models. The existence of the unsymmetrical bridging mode in the d^0 molybdenum and tungsten imido-bridged complexes Ia,b is of some interest. One very apparent reason for the unsymmetrical bridging is that each tungsten atom has one bridging nitrogen atom in a locally equatorial site and the other bridging nitrogen atom in a locally axial site; significantly different W–N bridge separations are therefore expected. However, this does not explain why molecules of compounds I adapt this particular overall structure. In particular, one could imagine an alternative structure of D_{2h} symmetry which would have axial methyl ligands and symmetrically bridging imido nitrogen atoms. This latter possibility is especially relevant in view of the symmetrically bridged compounds IIa,b, which also have the d^0 electronic configuration. In an effort to rationalize the existence

(17) Chisholm, M. H.; Cotton, F. A.; Extine, M.; Millar, M.; Stults, B. R. *J. Am. Chem. Soc.* **1976**, *98*, 4486–4491 and references therein.

Table V. Positional and Thermal Parameters for the Atoms of Ib, $[(CH_3)_2(t\text{-BuN})W]_2(\mu\text{-}t\text{-BuN})_2$, with Their Estimated Standard Deviations

atom	x	y	z	B(1,1)[a]	B(2,2)	B(3,3)	B(1,2)	B(1,3)	B(2,3)
W	0.54155 (2)	0.37307 (3)	0.43875 (2)	0.00308 (1)	0.00586 (2)	0.00519 (2)	−0.00017 (4)	0.00078 (2)	0.00235 (5)
N(1)	0.5643 (4)	0.2750 (6)	0.3173 (5)	0.0040 (3)	0.0070 (6)	0.0062 (5)	−0.0008 (8)	0.0017 (6)	0.0025 (9)
N(2)	0.4692 (4)	0.5343 (6)	0.3768 (5)	0.0033 (3)	0.0064 (6)	0.0057 (5)	0.0010 (7)	0.0007 (6)	0.0032 (9)
C(1)	0.7087 (6)	0.4155 (8)	0.5097 (7)	0.0049 (4)	0.0104 (9)	0.0076 (7)	−0.0003 (10)	0.0025 (9)	0.001 (1)
C(2)	0.4312 (5)	0.2178 (7)	0.4778 (7)	0.0044 (4)	0.0073 (7)	0.0081 (7)	−0.0029 (9)	0.0022 (8)	0.002 (1)
C(11)	0.5938 (6)	0.1719 (7)	0.2342 (7)	0.0052 (4)	0.0089 (8)	0.0073 (7)	0.0009 (10)	0.0030 (9)	0.000 (1)
C(12)	0.6364 (9)	0.2461 (10)	0.1390 (8)	0.0245 (10)	0.0110 (11)	0.0111 (8)	0.0025 (19)	0.0245 (12)	0.001 (2)
C(13)	0.6789 (8)	0.0759 (10)	0.3112 (9)	0.0125 (7)	0.0184 (13)	0.0099 (9)	0.0165 (15)	0.0071 (13)	−0.001 (2)
C(14)	0.4979 (9)	0.0860 (11)	0.1762 (12)	0.0088 (8)	0.0223 (14)	0.0302 (16)	−0.0059 (18)	0.0072 (18)	−0.038 (2)
C(21)	0.4309 (6)	0.5937 (7)	0.2515 (6)	0.0051 (4)	0.0074 (8)	0.0057 (6)	0.0006 (9)	−0.0005 (8)	0.002 (1)
C(22)	0.3676 (7)	0.7301 (8)	0.2553 (8)	0.0072 (6)	0.0100 (9)	0.0084 (8)	0.0036 (13)	−0.0011 (11)	0.007 (1)
C(23)	0.5265 (6)	0.6252 (9)	0.1994 (7)	0.0070 (5)	0.0139 (9)	0.0079 (7)	0.0019 (15)	0.0033 (9)	0.011 (2)
C(24)	0.3585 (6)	0.4881 (8)	0.1696 (8)	0.0070 (6)	0.0108 (9)	0.0076 (8)	0.0006 (13)	−0.0031 (12)	0.002 (2)

[a] The form of the anisotropic thermal parameter is $\exp[-(B(1,1)h^2 + B(2,2)k^2 + B(3,3)l^2 + B(1,2)hk + B(1,3)hl + B(2,3)kl)]$.

Table VI. Positional and Thermal Parameters for the Atoms of IIb, $[((CH_3)_2N)_2Ti]_2(\mu\text{-}t\text{-BuN})_2$

atom	x	y	z	B(1,1)[a]	B(2,2)	B(3,3)	B(1,2)	B(1,3)	B(2,3)
Ti	0.15955 (4)	0.02129 (3)	0.06557 (5)	0.00640 (3)	0.00214 (1)	0.01066 (5)	−0.00027 (5)	0.00558 (6)	0.00000 (6)
N(1)	−0.0131 (2)	0.0434 (1)	0.1206 (2)	0.0083 (2)	0.00210 (7)	0.0104 (2)	0.0000 (2)	0.0079 (3)	−0.0005 (2)
N(2)	0.3261 (2)	−0.0429 (1)	0.2309 (2)	0.0082 (2)	0.00326 (9)	0.0127 (3)	0.0015 (2)	0.0062 (4)	0.0019 (3)
N(3)	0.2390 (2)	0.1185 (1)	0.0015 (2)	0.0086 (2)	0.00267 (8)	0.0147 (3)	−0.0013 (2)	0.0083 (4)	0.0009 (3)
C(1)	−0.0382 (3)	0.1145 (1)	0.2140 (3)	0.0114 (3)	0.0028 (1)	0.0138 (3)	−0.0006 (3)	0.0120 (5)	−0.0027 (3)
C(2)	−0.1616 (3)	0.0897 (2)	0.2742 (3)	0.0198 (4)	0.0056 (2)	0.0274 (5)	−0.0012 (4)	0.0323 (5)	−0.0064 (5)
C(3)	−0.0949 (4)	0.1903 (2)	0.0996 (4)	0.0254 (5)	0.0028 (1)	0.0230 (5)	0.0034 (4)	0.0208 (7)	−0.0028 (4)
C(4)	0.1134 (3)	0.1361 (2)	0.3643 (3)	0.0170 (4)	0.0055 (1)	0.0182 (5)	−0.0016 (4)	0.0092 (7)	−0.0094 (4)
C(5)	0.4718 (3)	−0.0566 (2)	0.2164 (4)	0.0118 (3)	0.0054 (1)	0.0237 (5)	0.0050 (4)	0.0137 (6)	0.0033 (5)
C(6)	0.3221 (3)	−0.0916 (2)	0.3675 (4)	0.0187 (4)	0.0057 (2)	0.0215 (5)	0.0046 (4)	0.0187 (7)	0.0087 (5)
C(7)	0.3777 (3)	0.1643 (2)	0.1133 (4)	0.0131 (4)	0.0036 (1)	0.0234 (5)	−0.0036 (4)	0.0113 (7)	−0.0018 (4)
C(8)	0.1640 (3)	0.1605 (2)	−0.1590 (4)	0.0159 (4)	0.0048 (1)	0.0205 (5)	−0.0021 (4)	0.0087 (7)	0.0079 (4)

[a] The form of the anisotropic thermal parameter is $\exp[-(B(1,1)h^2 + B(2,2)k^2 + B(3,3)l^2 + B(1,2)hk + B(1,3)hl + B(2,3)kl)]$.

Chart II

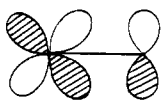

Chart III

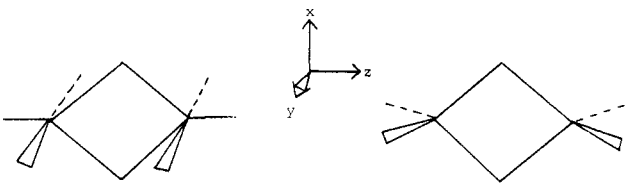

Chart IV

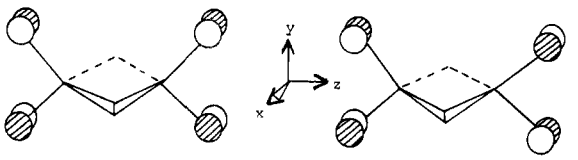

of unsymmetrical bridging in Ia,b, we have studied the electronic structures of model compounds with extended Hückel calculations. We have found that the structural differences between compounds I and II are a manifestation of inherent electronic differences which are established by the different overall π-bonding networks.[18]

A logical and convenient point at which to begin our analysis is a description of the bridge bonding in a simple Hückel framework. To do this, we will initially make, in addition to the usual approximations of the simple Hückel treatment of π systems, the following explicit assumptions, some of which will be amended later. (a) The metal d orbitals and the nitrogen p orbitals will have the same ionization potential, α, which as usual will be set equal to zero. (b) The metal s and p orbitals will not be taken into account nor will metal to terminal ligand σ bonds. (c) The complexes will initially be assumed to have the idealized symmetry of the point group D_{2h}. In the course of our analysis we will find that the resulting electronic structure of compounds I will demand a distortion to the observed lower symmetry. (d) The N(bridging)–metal–N(bridging) angles in I and II will be taken to be 90°, as will the N(terminal)–metal–N(terminal) angles in II. (e) The ideal π-bonding interaction between a metal d orbital and a nitrogen p orbital (Chart II) will be defined as β, an intrinsically negative number. The coordinate system we will be using throughout is drawn below in Chart III. In both D_{2h} and C_{2h} (the symmetry of the localized bonding system) the molecular plane, xz, is a symmetry plane, and our Hückel arguments will be confined to π orbitals which are antisymmetric to this plane.

Consider first the orbitals of the bridging region alone. These are the d_{xy} and d_{yz} orbitals of the two metal atoms and the p_y orbitals of the bridging nitrogen atoms. Caution must be used in the construction of the Hamiltonian; for example, note that—as a result of assumptions d and e above—the bonding interaction between the d_{xy} orbital of either metal atom and the p_y orbital of a bridging nitrogen atom is *not* β but rather $(2^{1/2}/2)\beta$ (in absolute magnitude). The resulting wave functions and energy levels are schematically illustrated in the center of Figure 3. Note that, in the absence of π-bonding terminal ligands, a closed-shell, delocalized, "aromatic" bridge-bonding system would be achieved if there were a total of four electrons present in the π orbitals considered here (see Figure 3, center). Just such a four-electron system, $Nb_2(CH_2SiMe_3)_4(\mu\text{-}CSiMe_3)_2$, was reported some time ago by Wilkinson and co-workers[19] and has essentially symmetrical bonding in the bridging region.[19a]

The symmetrically bridged compounds II are modeled by including the terminal amido nitrogen p_x orbitals in the Hamiltonian.

(18) There are minor differences between I and II in the bridging region σ bonds, but from the calculations they do not appear to be responsible for the gross structural differences.

(19) (a) Huz, F.; Mowat, W.; Skapski, A. C.; Wilkinson, G. *J. Chem. Soc., Chem. Commun.* **1971**, 1477–1478. (b) Mowat, W.; Wilkinson, G. *J. Chem. Soc., Dalton Trans.* **1973**, 1120–1124.

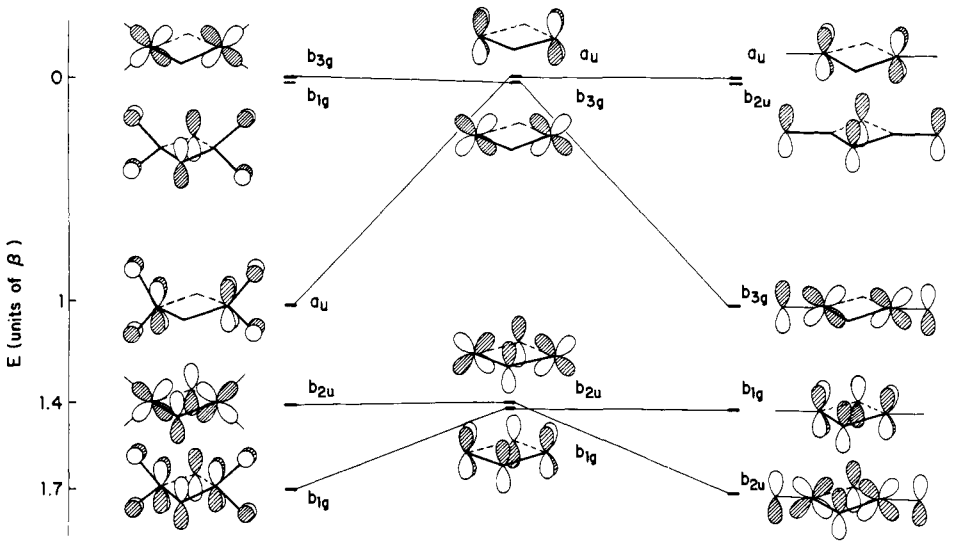

Figure 3. Center: Hückel π orbitals for a hypothetical dimer with no terminal ligand interactions. Only bonding and nonbonding orbitals are included. Two antibonding orbitals are not shown. Left: Hückel π orbitals for compounds II, with terminal π-ligand interactions included. Again only bonding and nonbonding orbitals of π symmetry are shown. Two "nonbonding" orbitals of σ symmetry and three antibonding orbitals of π symmetry are omitted. Right: Hückel π orbitals for compounds I, with terminal π-ligand interactions included. Again only bonding and nonbonding orbitals of π symmetry are shown.

While there are four symmetry-adapted linear combinations of these p_x orbitals, only two of them, a and b in Chart IV, are of the correct symmetry (b_{1g} and a_u, respectively) to interact with the π orbitals; the other two symmetry-adapted linear combinations are symmetric to the xz plane and are included in the σ framework. The effect of including the two symmetry combinations (a and b, Chart IV) in our model Hamiltonian is shown in the left side of Figure 3. Now there are four electron pairs to be accommodated in the Hückel π molecular orbitals: Two electron pairs have come from the p_y orbitals of the bridging imido nitrogen atoms and two electron pairs from the p_x orbitals of the terminal amido nitrogen atoms. (The terminal amido nitrogen atoms actually bear a total of four electron pairs, but two pairs are retained in orbitals of σ symmetry and are not considered further.) At first glance it appears that there will be a half-filled degenerate pair of MO's at the nonbonding energy level and a resulting "antiaromatic" system inconsistent with our assumed symmetric model. Put in another way, a near degenerate HOMO–LUMO pair strongly suggests a second-order Jahn–Teller distortion toward lower symmetry.[20]

If our simple model is predicting "antiaromatic" character for the compounds II, why then are they observed to be symmetric? We can answer this question by considering two factors which we have hitherto specifically neglected. First, the assumption that the metal d orbitals and the nitrogen p orbitals have equal ionization potentials must be revised. Even in these compounds, where the metal atom exists in a *formal* d^0, high-oxidation state and the bridging imido nitrogen atoms in formal −2 oxidation states, a much more reasonable assumption is that the appropriate ionization potential for a metal d orbital is at least 1 eV less binding than the ionization potential of a nitrogen p orbital. This factor alone will break the present degeneracy of the HOMO(b_{1g})–LUMO(b_{3g}) pair, since the HOMO is confined entirely to the nitrogen atoms and the LUMO to the metals. Creating a sizable gap between the HOMO and LUMO will lessen the driving force for a second-order Jahn–Teller distortion from the symmetric structure.

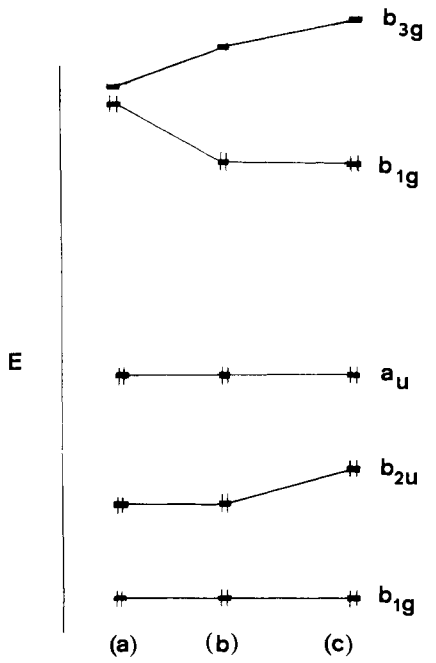

Figure 4. (a) Unperturbed π orbitals of compounds II. (b) The π orbitals of compounds II after raising the H_{ii} values for the metal d orbitals and lowering the H_{ii} values for the nitrogen p orbitals (schematic). (c) The π orbitals of compounds II after the further perturbation of including terminal ligand σ repulsion.

Chart V

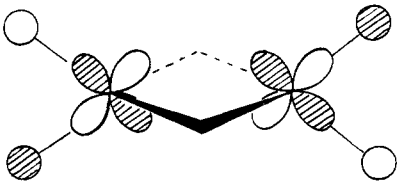

The second factor we must consider is the effect the terminal ligand–metal σ orbitals might have on the π framework. In compounds IIa,b the terminal amido nitrogen atom "sp^2 lone-pair" σ orbitals span the irreducible representations a_g, b_{1u}, b_{2u}, and b_{3g}. The a_g and b_{1u} lone-pair combinations cannot interact with the π framework, but the b_{2u} and b_{3g} combinations interact strongly

(20) (a) Den Boer, P. H. W.; Den Boer, P. C.; Longuet-Higgins, H. C. *Mol. Phys.* **1962**, *5*, 387–390. Nicholson, B. J.; Longuet-Higgins, H. C. *Ibid.* **1965**, *9*, 461–472. (b) Bader, R. F. W. *Mol. Phys.* **1960**, *3*, 137–151. *Can. J. Chem.* **1962**, *40*, 1164–1175. (c) Bartell, L. S. *J. Chem. Educ.* **1968**, *45*, 754–767. Bartell, L. S.; Gavin, R. M., Jr. *J. Chem. Phys.* **1968**, *48*, 2466–2483. (d) Salem, L. *Chem. Phys. Lett.* **1969**, *3*, 99–101. Salem, L.; Wright, J. S. *J. Am. Chem. Soc.* **1969**, *91*, 5947–5955. Salem, L. *Chem. Brit.* **1969**, *5*, 449–458. (e) Pearson, R. G. *J. Am. Chem. Soc.* **1969**, *91*, 1252–1254, 4947–4955. (f) Pearson, R. G. "Symmetry Rules for Chemical Reactions"; Wiley-Interscience: New York, 1976.

Chart VI

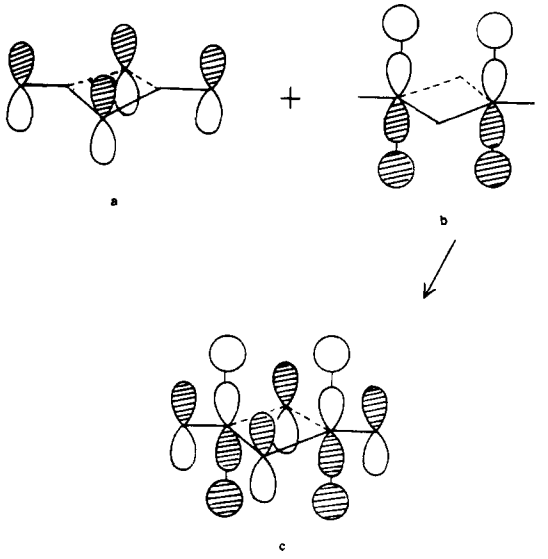

with the appropriate π orbitals. The result is a significant destablilization of the LUMO, the b_{3g} orbital (Chart V), and the energy gap between HOMO and LUMO is made even more substantial by this effect. These two factors are schematically illustrated in Figure 4.

Now consider the model for compounds Ia,b. Including the p_y orbitals of the terminal imido nitrogen atoms in the Hückel Hamiltonian results in the energy levels and wave functions shown in the right side of Figure 3. Significantly, the energy levels turn out to be the same as those in our model for compounds II (Figure 3, left), but the wave functions are different. There are again four electron pairs to be accommodated, and there is again a degenerate HOMO–LUMO pair. And again, making the nitrogen p ionization potentials more binding than the metal d orbitals results in a splitting of the degeneracy. This time, however, the LUMO is of a symmetry (a_u) which is not matched by *any* ligand σ orbital (in the point group D_{2h}) and consequently remains at significantly low energy. The HOMO, of b_{2u} symmetry (a in Chart VI), is repelled by a ligand σ combination of the same symmetry (b and c in Chart VI). Consequently, the effect of the terminal ligand σ bonds is a *lessening* of the HOMO–LUMO gap; see Figure 5.

We have thus arrived at the significant difference between compounds I and II, insofar as π effects are concerned.[18] Both compounds have a π-bonding topology which results in a near degenerate HOMO–LUMO pair, separated only by the difference in the ionization potentials of the nitrogen p and metal d atomic orbitals. In I, the terminal ligand σ orbitals interact with, and repel, the HOMO, resulting in a very small HOMO–LUMO gap. In such a situation there is a driving force for a distortion from the high symmetry which will permit mixing of the HOMO and LUMO, resulting in significant stabilization of the HOMO and the overall molecule. The terminal σ orbitals of compounds II, however, interact only with the LUMO, and the resulting HOMO–LUMO gap is much larger than that of I. A distortion from the high symmetry will still permit HOMO–LUMO mixing, but such mixing, now between orbitals of greatly different energies, results in little if any stabilization of the HOMO, and interactions among other orbitals oblige the molecule to retain its high symmetry.

Extended Hückel calculations[21] on models for these systems

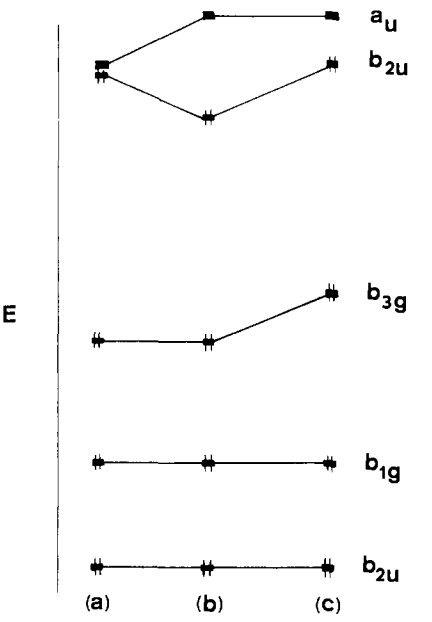

Figure 5. (a) Unperturbed π orbitals of compounds I. (b) The π orbitals of compounds I after raising the H_{ii} values for the metal d orbitals and lowering the H_{ii} values for the nitrogen p orbitals (schematic). (c) The π orbitals of compounds I after the further perturbation of including terminal ligand σ repulsion.

support the basic agruments we have presented. (The parameters are discussed in the Appendix.) A difficulty we have encountered is that in these d^0 complexes there are no filled orbital–filled orbital repulsive interactions between the metal and bridging nitrogen atoms. In the absence of two-body repulsion we find that—if a reasonable metal–metal separation is maintained—the bridging region of both complexes I and II optimizes to a nonsymmetrical structure, simply because the optimum metal–nitrogen separation is very short. With the inclusion of two-body repulsive forces,[21] the computational method qualitatively reproduces the experimental geometries.

Our analysis of the source of the distortion from high symmetry in compound I rests on the necessary presence of a small HOMO–LUMO gap in the symmetrical model structures. Mixing between HOMO and LUMO results, however, not only from distortions in the bridging region but also from motions of the terminal ligands, as illustrated in Chart VII below. This accounts, qualitatively, for the overall structures observed for compounds Ia,b.

The observed structures of compounds II do not have ideal D_{2h} symmetry despite the symmetrical bridge bonding. The bridging nitrogen atoms are distinctly pyramidal. In I, in contrast, the bridging nitrogen atoms are planar (they lie in the plane defined by the two metal atoms and C(21)). The pyramidality of the bridging nitrogen atoms of II can be rationalized by noting that, in the symmetrical structure, the HOMO of II (b_{1g}, sketched in Figure 3, left) is confined to the nitrogen atoms without any metal participation. Hence there remains a certain amount of "lone-pair" character at the nitrogen atoms, and pyramidalization is not unreasonable.[22] In compounds I, in contrast, the HOMO (after the distortion!) is partially N(bridge)–metal bonding and the tendency toward pyramidalization is suppressed. Similarly, in organic amide compounds pyramidalization is not commonly observed because of π interaction with the CO π^* orbital and partial multiple-bond formation.

Extensions. Given the arguments that have been presented in the previous section, the following predictions can be ventured. If a compound could be prepared having the same basic structure as I but having axial terminal ligands with good π-donor capability,

(21) Pensak, D. A.; McKinney, R. J. *Inorg. Chem.* **1979**, *18*, 3407–3413. McKinney, R. J.; Pensak, D. A. *Inorg. Chem.* **1979**, *18*, 3413–3417 and references therein. The theoretical basis for the two-body repulsion forces is from Anderson, A. B. *J. Chem. Phys.* **1975**, *62*, 1187–1188. The resulting modifications to the extended Hückel method have also originated with Anderson and have been applied to other problems involving transition-metal dimers. See, for example: Anderson, A. B. *Inorg. Chem.* **1976**, *15*, 2598–2602 and references therein; *J. Am. Chem. Soc.* **1978**, *100*, 1153–1159 and references therein.

(22) Levin, C. C. *J. Am. Chem. Soc.* **1975**, *97*, 5649–5655 and references therein. Cherry, W.; Epiotis, N. *Ibid.* **1976**, *98*, 1135–1140 and references therein.

Table VII. Extended Hückel Parameters

	s			p			d					
	n	ζ	H_{ii}	n	ζ	H_{ii}	n	C_1	ζ_1	C_2	ζ_2	H_{ii}
Zr	5	1.82	−10.10	5	1.78	−6.86	4	0.6210	3.84	0.5790	1.51	−12.10
Mo	5	1.96	−10.10	5	1.90	−6.86	4	0.5899	4.54	0.5899	1.90	−12.10
N	2	1.92	−20.30	2	1.92	−13.40						
H	1	1.30	−13.6									

Chart VII

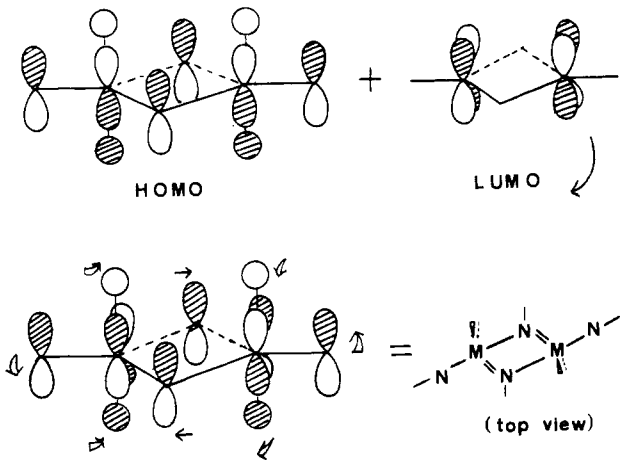

the LUMO of the symmetrical structure would be significantly raised by repulsion of the π donors. The HOMO–LUMO gap would therefore be greater than that in I, the driving tendency for distortion thereby lessened, and the molecule might adopt a more nearly symmetrical structure. Conversely, an analogue of II with less strongly σ-donating terminal ligands would have a smaller HOMO–LUMO gap than II and might begin to show a distortion in the bridging region.

An interesting possibility is that the existence of unsymmetrically bridging CO groups[23] may be paritally due to electronic effects similar to those examined in the present paper.

Also related to the present compounds I and II are the unsymmetrically bridged molybdenum and tungsten compounds recently reported by Chisholm, Cotton, and co-workers.[24] These latter compounds, however, contain d electrons, which reside in molecular orbitals that are empty in compounds I and II and which have geometric preferences we have not yet studied.

Summary and Conclusions

From simple and extended Hückel models for the two different imido-bridged metal dimer systems I and II we have been able to explain their appreciably different structures. In particular, the marked asymmetry in compounds I is the result of a second-order Jahn–Teller distortion not unlike the localization of bonding expected for antiaromatic cyclic hydrocarbons (C_4H_4,[25] C_8H_8); such a distortion is absent in the symmetrically bridged compounds II. The observed difference between the two compounds is a manifestation of their inherently different π- and σ-bonding topologies and is independent of our computational method or parameterization.

Acknowledgment. We wish to express our gratitude to Dr. D. A. Pensak and Dr. R. J. McKinney for assistance with use of the TRIBBLE computational package on the Du Pont computer facilities.[21] We also wish to acknowledge helpful comments by Professor R. Hoffmann of Cornell University. Hückel calculations were performed by using a program kindly provided by Dr. S. Russo of Cornell University.

Appendix

Extended Hückel calculations have been performed on the hypothetical compounds $[(H_2N)_2Zr]_2(\mu\text{-}NH)_2$ (a model for IIa) and $[H_2(NH)Mo]_2(\mu\text{-}NH)_2$ (a model for Ia). The parameters used for Mo are from the work of Summerville and Hoffmann,[12b] and we list them in Table VII. We have deliberately equated the H_{ii} values for Mo and Zr to the value used by Summerville and Hoffmann[12b] for Nb to minimize the effect of parameter differences in our analysis. It will be noted that if Mo were more electronegative than Zr (the intuitive expectation), the result would be a reinforcement of the trends we have analyzed. Exponents for Zr are taken from the paper by Basch and Gray.[26]

As discussed in the text there is an unfortunate tendency for the metal–nitrogen separation to optimize at chemically unreasonable distances. The inclusion of the explicit two-body repulsive forces[21] largely but not entirely overcomes this tendency. Even with their inclusion, we have found that systems I and II both optimize with nonsymmetric bridging geometries if the experimental metal–metal separations (approximately 3.09 Å) are retained. This is because the optimum metal–nitrogen separation—with this method and this parameterization—is noticeably less than the average distance of approximately 2.06 Å found experimentally. However, by shortening the metal–metal separation to 2.66 Å (the computed optimum), the metal-bridging nitrogen distances are sufficiently close to optimum that the observed geometries of I and II are qualitatively reproduced. The trends we have presented and analyzed in the text are definitely present in all our calculations, regardless of the metal–metal separation used.

Supplementary Material Available: A listing of observed and calculated structure factor amplitudes, a listing of hydrogen atom positions, and (for IIb only) a table of least-squares planes (35 pages). Ordering information is given on any current masthead page.

(23) A beautiful example of the occurrence of unsymmetrically bridging CO ligands, in a compound which intuitively could have higher symmetry, has been published by: Knox, S. A. R.; Stansfield, R. F. D.; Stone, F. G. A.; Winter, M. J.; Woodward, P. *J. Chem. Soc., Chem. Commun.* **1979**, 934–936.

(24) Chisholm, M. H.; Cotton, F. A.; Extine, M. W.; Kelly, R. L. *J. Am. Chem. Soc.* **1978**, *100*, 3354–3358. Chisholm, M. H.; Cotton, F. A.; Extine, M. W.; Murillo, C. A. *Inorg. Chem.* **1978**, *17*, 696–698.

(25) A recent structure of a symmetrically-substituted cyclobutadiene (Irngartinger, H.; Riegler, N.; Malsch, K.-D.; Schneider, K.-A.; Maier, G. *Angew. Chem.* **1980**, *92*, 214–215) reveals it to have nearly equal C–C bond lengths. For a theoretical explanation of this see: Borden, W. T. *J. Am. Chem. Soc.* **1975**, *97*, 5968–5970 and references therein.

(26) Basch, H.; Gray, H. B. *Theor. Chim. Acta* **1967**, *4*, 367–376.